CHAPTER IV
RESULTS AND DISCUSSION

This chapter presents the effect of bimetallic catalysts (Pd and Pt on Y-zeolite) on waste tire pyrolysis. Metal ratio and catalyst preparation method were the studied parameters on the qualities and quantities of the pyrolytic products.

Table 4.1 Physical and chemical properties of Y-zeolite (Tosoh Company)

Property	Value
Cation type	H
SiO_2/Al_2O_3 (mol/mol)	15
NH_3-TPD (mmol/g)	<0.1
Surface area (m^2/g)	600
Crystal size (μm)	0.2-0.4
Mean particle size (μm)	6-8

The bimetallic catalysts that were used were also prepared according to the following three methods: (i) co-impregnation of Y-zeolite with a solution of both metal precursors: symbol = Pd-Pt/Y; (ii) successive impregnation in which Pd is first loaded followed by Pt: symbol = Pd*-Pt/Y (the asterisk indicates the metal impregnated first); (iii) successive impregnation in which Pt is first loaded followed by Pd: symbol = Pd-Pt*/Y. All catalyst preparation methods had a fixed total metal loading of 1 %wt and the weight of Pd per weight of total metals (α_{Pd}) was varied at 0, 0.2, 0.4, 0.6, 0.8, and 1, as shown in the Table 4.2. The amount of metal loading for every sample catalysts was determined by using AAS, as shown in Table G1. The result shows that sample catalysts have the amount of metal loading closely to the desired number. The physical and chemical properties of Y-zeolite are shown in Table 4.1.

Table 4.2 Catalyst samples in this work

α_{Pd} / Samples	0	0.2	0.4	0.6	0.8	1
Pt/Y	●					
Pd/Y						●
Pd-Pt/Y		●	●	●	●	
Pd*-Pt/Y		●	●	●	●	
Pd-Pt*/Y		●	●	●	●	

Note: $\alpha_{Pt} = \dfrac{wt_{Pt}}{wt_{Metals}}$; $\alpha_{Pd} = \dfrac{wt_{Pd}}{wt_{Metals}}$; $wt_{Metals} = wt_{Pt} + wt_{Pd}$

$\alpha_{Pt} = 1 - \alpha_{Pd}$; $\alpha_{Pd} = 1 - \alpha_{Pt}$

4.1 Effect of Preparation and Metal Ratio on Pyrolysis Products

This research focused on two effects, which were metal ratio (α_{Pd}) and catalyst preparation method (co-impregnation and successive impregnation). This section presents the quality and quantity of pyrolytic products obtained from varying several parameters of the bimetallic catalyst. An appropriate metal ratio and a catalyst preparation method suitable for the production of the high quality products were determined.
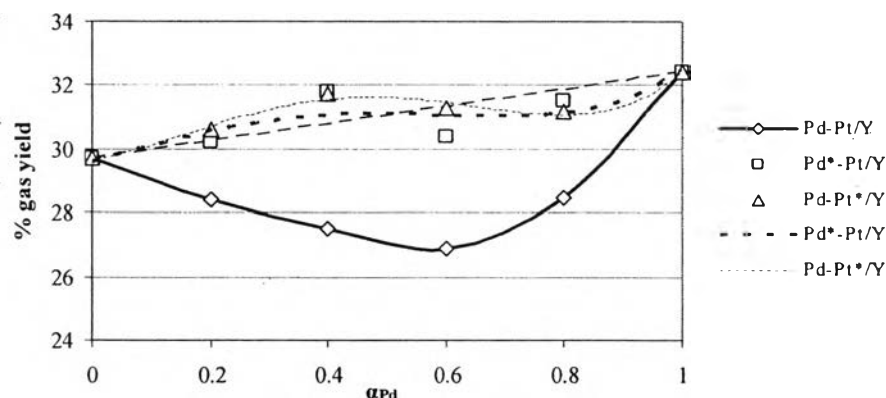
4.1.1 Product Yield

Waste tire pyrolysis is a thermal decomposition process that decomposes the polymer chains of tire. This work used an autoclave reactor for the pyrolysis to produce a solid fraction, a liquid fraction, and a gas fraction. A pyrolysis temperature of 500 °C gives the complete pyrolysis. Pyrolysis without a catalyst generates solid yield, liquid yield, and gas yield of about 45 %, 32 %, and 22 %, respectively. Using Y-zeolite for catalytic pyrolysis decreased liquid yield and increased gas yield because Y-zeolite is an acid catalyst, which can help to improve hydrocarbon cracking from waste tire decomposition (William and Brindle, 2002).

The liquid yield of pyrolysis with Pd/Y or Pt/Y catalyst was lower than pyrolysis with and without Y-zeolite because the loading of Pd or Pt on the Y-zeolite enhanced the cracking reaction (Chusuton, 2007).
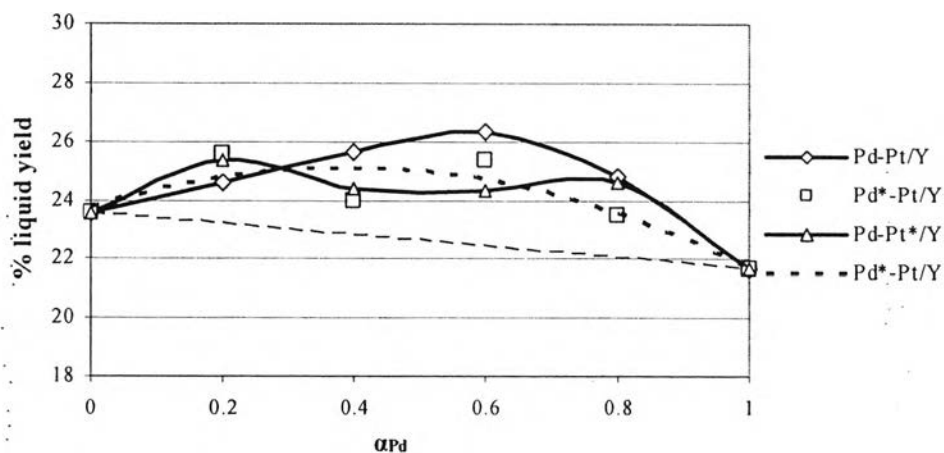
(a)

(b)

Figure 4.1 Effect of metal ratio and catalyst preparation on (a) liquid product yield and (b) gas product yield.

The liquid product yield of bimetallic catalysts at any ratio and catalyst preparation is shown in Figure 4.1a. It can be seen that the bimetallic catalysts have a synergistic effect on the liquid yield as compared with the monometallic catalysts ($\alpha_{Pd} = 0$ or 1). Almost of the co-impregnated catalysts give a higher liquid yield than successive impregnated catalysts, except at $\alpha_{Pd} = 0.2$.

The liquid yield of Pd-Pt/Y catalysts increases with the increasing amount of Pd (α_{Pd}), and gives the highest liquid yield at α_{Pd} = 0.6 (26.32 %), and then liquid yield decreases when α_{Pd} increases up to 0.8. The liquid yield of the Pd*-Pt/Y catalysts slightly increases with increasing α_{Pd}. And, α_{Pd} = 0.4 gives the highest liquid yield (25.57 %). The catalyst prepared by successive impregnation with loading Pt first at α_{Pd} = 0.2 provides the highest liquid yield (25.38 %). After that, the increasing α_{Pd} to 0.6 makes the yield slightly decrease to the value about 24 %, and then the yield slightly increases again to 25 % at α_{Pd} = 0.8.

From the results, it can be suggested that loading two metals on the catalyst slightly decrease the cracking activity of the catalyst, although the total metal loading is only 1 %wt. So, the effect of decreasing acid site by metal loading can be neglected. However, the liquid yield of all bimetallic catalysts is insignificantly different (1 – 5 %). It can be suggested that using two metals has a little effect on reducing the cracking activity of the catalysts. Using the Pd-Pt/Y catalyst at α_{Pd} = 0.6 gives the highest yield of liquid product as compared to all of the catalysts. The quality of liquid product can be revealed from the quantity of chemical compositions in oil such as saturated hydrocarbon compounds, aromatic compounds, and petroleum fractions (naphtha fraction).

The gas yield of all catalysts is in the opposite trend to the liquid yield (Figure 4.1b). It means that the gas products are generated from the cracking of hydrocarbon molecules to the low carbon number molecules (C_1-C_8) which some can not be condensable. The bimetallic catalysts produce the low amount of gas yield. And the co-impregnated catalysts give a lowest gas yield, especially at α_{Pd} = 0.6. Using the Pd/Y catalyst produces the highest gas yield (32 %).

4.1.2 Chemical compositions in oils

Maltene were separated into 5 chemical compositions (saturated hydrocarbon, mono-, di-, poly-, and polar-aromatic compounds) by liquid adsorption chromatography using various mobile solvents (Sebor *et al.*, 1999). Each composition can roughly indicate the quality of the oil products. For example, the high amount of saturated hydrocarbons in oil is needed, especially for naphtha and diesel fuels. The high amount of mono-aromatics in the pyrolytic oil is desired to be

used as petrochemical feed stock. And, the low amount of polar-aromatics emits low polluted gas.

Appendix B presents that using Y-zeolite gives the higher amount of saturated HCs and mono-aromatics than without a catalyst because catalytic pyrolysis with Y-zeolite is suitable to produce mono-aromatics (benzene, toluene, and mixed xylene) (Williams and Brindle, 2003). Acid zeolite can also produce saturated hydrocarbon compounds.

The saturated hydrocarbon compounds are the main components in diesel fuel. Using Pd-Pt bimetallic catalysts can improve the yield of saturated hydrocarbon compounds in the liquid product (Jaqquin et al., 2004). The Pd and Pt have generally high both activity of hydrogenation and hydrogenolysis reaction (Rousset et al., 2000). So, the bimetallic (Pd-Pt) catalysts can help to drive aromatic hydrogenation and ring-opening reaction.
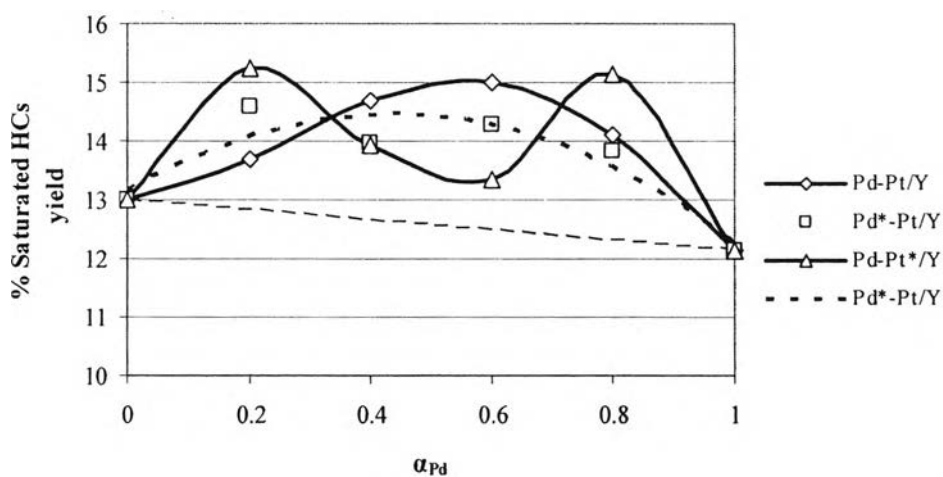

Figure 4.2 Effect of metal ratio and catalyst preparation on saturated hydrocarbon yield in the oil products.

Figure 4.2 shows the synergism between the two metals, which has the effect on the saturated hydrocarbon yield. The saturated hydrocarbon yield of Pd-Pt/Y catalysts increases with the increasing Pd ratio (α_{Pd}), then reaches the highest yield at $\alpha_{Pd} = 0.6$ (15 %), and later decreases with increasing α_{Pd} up to 0.8. The saturated HC yield of Pd*-Pt/Y catalysts has similar trend to the Pd-Pt/Y catalysts,

but the Pd*-Pt/Y catalysts give slightly lower yield than the Pd-Pt/Y catalysts, except at $\alpha_{Pd} = 0.2$. The highest saturated hydrocarbon yield of Pd*-Pt/Y catalyst is at $\alpha_{Pd} = 0.4$ (14.5%). However, the saturated hydrocarbon yield of Pd-Pt*/Y catalyst has a high number at $\alpha_{Pd} = 0.2$ and 0.8. These catalysts produce the saturated HCs value of 15.2 % and 15.1 %, respectively.

The Pd-Pt*/Y catalysts at $\alpha_{Pd} = 0.2$ and 0.8 give the highest saturated hydrocarbon yield among the other types of the catalysts. It is expected that these catalysts have the high amount of active sites and high metal dispersion. The reasons can be supported by using H_2 chemisorption technique, which will be discussed in Section 4.2.2.

From the liquid product yield (Figure 4.1) and saturated hydrocarbon yield (Figure 4.2), it can be concluded that the Pd-Pt/Y catalyst at $\alpha_{Pd} = 0.6$ and the Pd-Pt*/Y catalysts at $\alpha_{Pd} = 0.2$ and 0.8 might be suitable to use in catalytic pyrolysis for the production of highly-stable oils because they produce the high amount of liquid yield with the high number of saturated hydrocarbon yield.
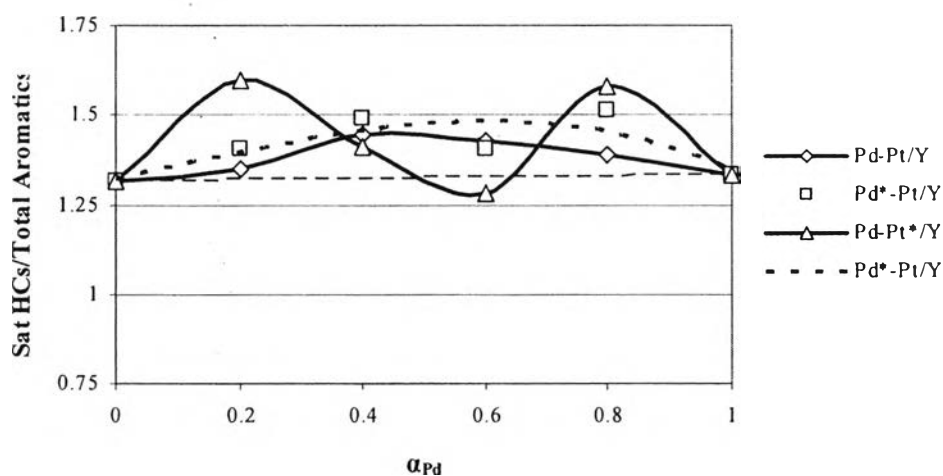

Figure 4.3 Effect of metal ratio and catalyst preparation on saturated hydrocarbons/total aromatics ratios.

The saturated hydrocarbons per total aromatics (the sum of mono-, di-, poly-, and polar-aromatics) ratio of catalysts is shown in Figure 4.3. It is found that all of the catalysts produce saturated hydrocarbons higher than total aromatics (ratio

value > 1). And, almost of the bimetallic catalysts give the higher ratio than the monometallic catalysts.

The saturated HCs/total aromatics ratio of Pd-Pt/Y catalysts increases with the increasing α_{Pd} up to 0.4. After that, the increasing α_{Pd} up to 0.8 the ratio value slightly decreases. The Pd*-Pt/Y catalysts give the similar trend to the Pd-Pt/Y catalysts. The saturated HCs/total aromatics ratios of Pd*-Pt/Y catalysts are higher than those of the Pd-Pt/Y catalyst. The Pd*-Pt/Y catalyst at $\alpha_{Pd} = 0.4$ gives the highest saturated HCs/total aromatics ratio (around 1.5). The Pd-Pt*/Y catalysts at $\alpha_{Pd} = 0.2$ and 0.8 give the highest saturated HCs/total aromatics ratio (nearly to 1.55) as compared to all of the catalysts.

The saturated HCs/total aromatics ratio of bimetallic catalysts is in the range of high values, which can imply that the bimetallic catalysts can increase the hydrogenation and hydrogenolysis activities (Niquille-Röthlisberger and Prins, 2006 and Pawalec et al., 2002). Then, some of the saturated HC compounds may come from aromatic hydrogenation and ring opening reaction.

Table 4.3 Amount of polar-aromatic compounds in the maltenes determined by liquid chromatography

Catalyst samples	α_{Pd}	%wt of polar-aromatic in maltenes
Noncatalyst	-	15.9
Y	-	12.1
Pd/Y	1	7.32
Pt/Y	0	7.66
Pd-Pt/Y	0.8	6.74
	0.6	6.33
	0.4	6.35
	0.2	6.68
Pd*-Pt/Y	0.8	6.74
	0.6	6.33
	0.4	6.44
	0.2	6.41
Pd-Pt*/Y	0.8	5.41
	0.6	6.25
	0.4	6.17
	0.2	5.83

The majority of polar-aromatic compounds in oil products is S-containing aromatics. S atoms are given off at the cross-links generated from vulcanization in tire production process. The low amount of polar-aromatics in an oil product indicates that the oil has high quality. The polar-aromatic yields of the monometallic catalysts are lower than those obtained from Y-zeolite and from noncatalytic case because the Pt/Y or Pd/Y catalysts can enhance the ring opening of the poly- and polar-aromatic hydrocarbons (Arribas and Martinez, 2002). Then, the

The polar-aromatic yields from the bimetallic catalysts are shown in Table 4.3. All of the bimetallic catalysts give the lower amount of polar-aromatics than the monometallic catalysts and without a catalyst (15.91 %). It can be suggested that the bimetallic catalysts have high hydrogenolysis activity for C-S-C bond breaking. The lowest amount of polar-aromatics obtained from using the Pd-Pt/Y catalysts is at α_{Pd} = 0.4 and 0.6. Both of them have the value of about 6.33 %. The lowest polar-aromatic yield of Pd*-Pt/Y catalyst is at α_{Pd} = 0.6 (6.33%). The Pd-Pt*/Y catalysts at any ratio give the lower amount of polar-aromatic compounds than the other types of bimetallic catalysts. α_{Pd} = 0.2 and 0.8 of the Pd-Pt*/Y catalysts have high catalytic activity, because they produce the oil with the very low amount of polar-aromatic yields. And the catalyst prepared by successive impregnation with loading Pt first at α_{Pd} = 0.2 give the lowest polar-aromatic production.
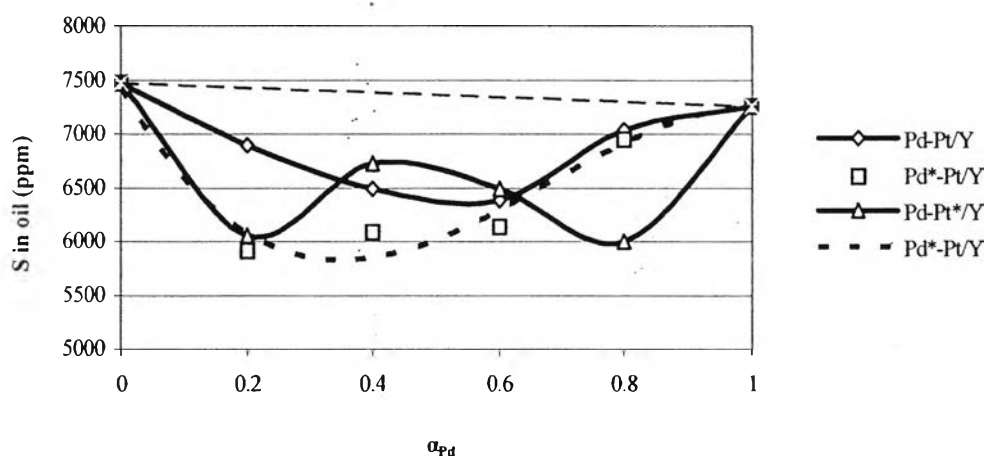

Figure 4.4 Effect of the bimetallic catalysts on the sulfur content in oil products.

The polar-aromatic in oil products were analyzed by using the elemental analysis technique to determine the amount of sulfur contents in oil products. And, the results show that the bimetallic catalysts give the oils with lower sulfur contents than the monometallic catalysts, as shown in Figure 4.4. It can be implied that the bimetallic catalysts have high C-S-C bond breaking activity to remove sulfur atoms from the oil products. The co-impregnated catalysts give the oil with the lowest sulfur content at α_{Pd} = 0.6. The co-impregnated catalysts give the higher sulfur contents in oil product than the successive impregnated catalysts. The

with the lowest sulfur content at $\alpha_{Pd} = 0.6$. The co-impregnated catalysts give the higher sulfur contents in oil product than the successive impregnated catalysts. The lowest amount of sulfur in the oil product of the Pd*-Pt/Y catalyst is at $\alpha_{Pd} = 0.2$. And, the Pd-Pt*/Y catalysts produce oil with the very low sulfur content at $\alpha_{Pd} = 0.2$ and 0.8.

As mentioned above, it is found that using the Pd-Pt*/Y catalysts at $\alpha_{Pd} = 0.2$ and 0.8 could give the highest stable oil, since they produce the oil with high saturated HCs yield and low amount of sulfur and aromatic contents.

### 4.1.3 Petroleum Fractions in Maltene

The maltene was also cut into five petroleum fractions: naphtha, kerosene, light gas oil, heavy gas oil, and long residue from the simulated true boiling point curves obtained from a Simulated Distillation Gas Chromatography. The amount of each fraction reveals the activity of the catalysts and the quality of the oil product.

The cracking activity of Y-zeolite can help to increase the yield of low molecular weight (low boiling point) compounds. So, the yield of naphtha and kerosene which have low boiling points (<200 °C, and 200 °C – 250 °C, respectively) can be increased by using an acid catalyst such as Y-zeolite. On the other hand, the amount of gas oil and long residue, which have high boiling point (250 – 370 °C, and >370 °C, respectively), can be cracked into low boiling point compounds because of the cracking activity of the acid catalyst. As mentioned earlier, the loading of Pt or Pd on the Y-zeolite can help to improve the cracking of high boiling point compounds into low boiling point compounds (Arribas *et al.*, 2002). Then, using the monometallic catalysts gives oil with the high amounts of naphtha and kerosene, and with the low amount of gas oil and long residue.

Using the bimetallic catalysts of Pt and Pd enhances the amount of naphtha yield in the oil product. These results suggest that the bimetallic catalysts can help to split of high boiling point compounds into naphtha fraction. The kerosene, gas oil, and long residue fractions, which have higher boiling points than naphtha, are produced with a very low yield when the bimetallic catalysts are used.
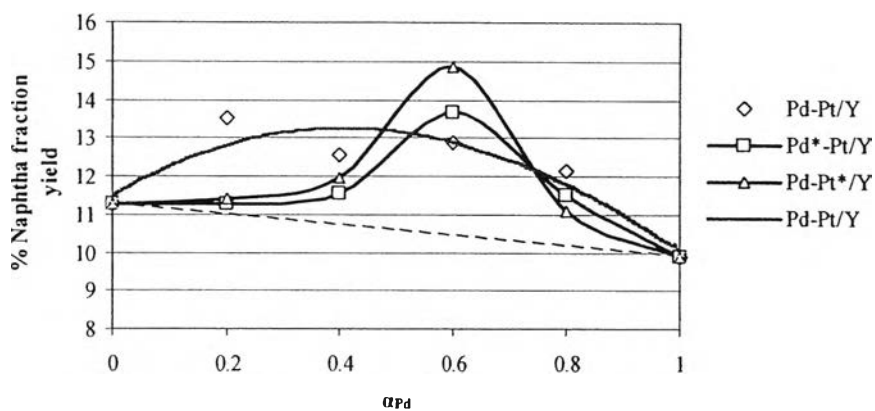
(a)
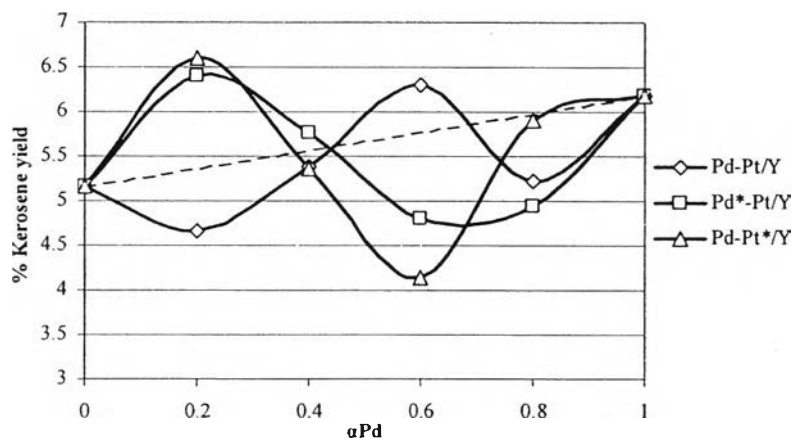
(b)
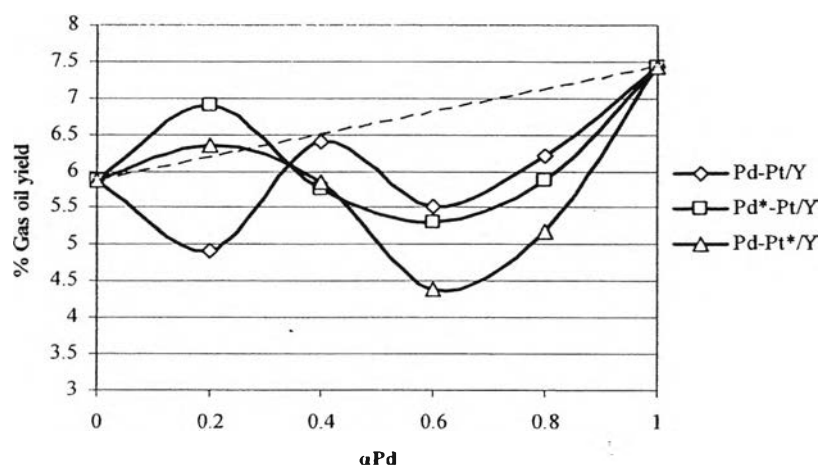
(c)

Figure 4.5 Effect of metal ratio and catalyst preparation on: **(a)** naphtha yield, **(b)** kerosene yield, and **(c)** gas oil yield in maltenes.

Figure 4.5 shows that there exists the synergistism between Pd and Pt, and it affects to the naphtha yield. The curves of kerosene and gas oil yield of bimetallic catalysts are wavy. The catalysts prepared by the co-impregnation method produce higher naphtha yield than those prepared by the successive impregnation methods, except at α_{Pd} = 0.6. The naphtha yield of Pd-Pt/Y catalysts increases with increasing α_{Pd}. The Pd-Pt/Y catalyst at α_{Pd} = 0.6 gives the moderate naphtha yield. This catalyst also gives the moderate kerosene and gas oil yield. The Pd*-Pt/Y and Pd-Pt*/Y catalysts provide the similar trend of naphtha yields. The naphtha yield from both preparation methods increases with the increasing α_{Pd}, and reaches the maximum at α_{Pd} = 0.6. The Pd*-Pt/Y catalyst at α_{Pd} = 0.2 gives the high amount of kerosene and gas oil yields, but it produces the low amount of naphtha yield. And, α_{Pd} = 0.2 of the Pd-Pt*/Y catalyst gives a high kerosene yield.

From the oil analysis results, the high catalytic activity of co-impregnated catalyst is at α_{Pd} = 0.6, but the Pd-Pt/Y catalyst at α_{Pd} = 0.6 gives lower catalytic activity than the Pd-Pt*/Y catalysts at α_{Pd} = 0.2 and 0.8. Therefore, the Pd-Pt*/Y catalysts at α_{Pd} = 0.2 and 0.8 produce the oil products with high saturated HCs and with very low sulfur and aromatic contents. This type of catalysts also produces the oil product with high kerosene fraction.

4.1.4 Light olefins and liquid petroleum gas

The pyrolytic gas was analyzed by using a GC. The details of results are given in Appendix F. This work is interested in the light olefins (ethylene and propylene) and LPG (60 % propane and 40 % mixed C_4) production. The light olefins has high price for chemical feedstock. The propane and mixed C_4 can be used as a fuel or cooking gas.
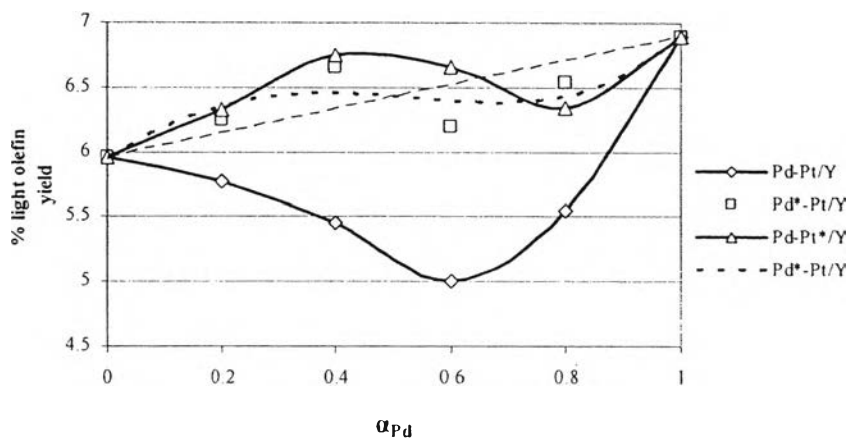
(a)
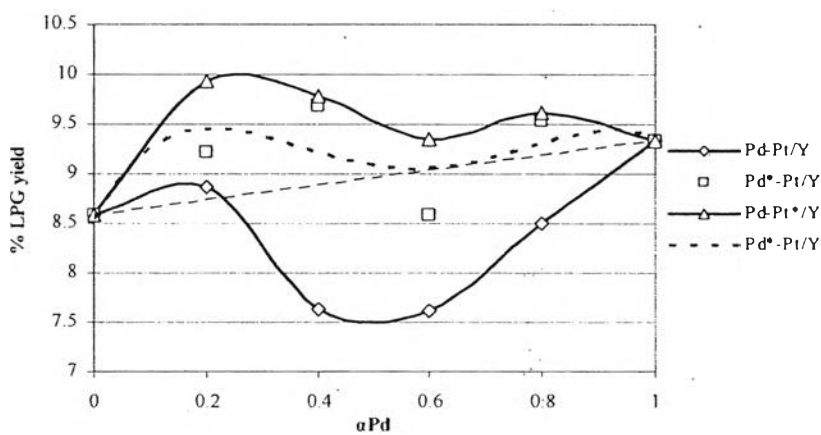
(b)

Figure 4.6 Effect of metal ratio and catalyst preparation on: **(a)** Light olefins, and **(b)** LPG yields.

As mentioned earlier, the gas yields of bimetallic catalysts are lower than those of the monometallic catalysts. The Pd/Y catalyst gives the highest gas yield, and also gives the highest yield of light olefins. Any ratio of the bimetallic catalysts produces the low amount of light olefins than the Pd/Y catalyst, especially the co-impregnated catalysts.

Figure 4.6a shows that any metal ratio of the Pd-Pt/Y catalysts gives the lower light olefins yield than the monometallic catalysts, especially $\alpha_{Pd} = 0.6$. The co-impregnated catalysts give a lower light olefin yield than the successive

impregnated catalysts. The light olefin yields of Pd*-Pt/Y catalysts are nearly constant (6.4 % – 6.45 %) with increasing α_{Pd}. The light olefin yields of Pd*-Pt/Y catalysts are higher than the Pt/Y catalyst, but is lower than the Pd/Y catalyst. The Pd-Pt*/Y catalysts are better than the other bimetallic catalysts. α_{Pd} = 0.4 and 0.6 of the Pd-Pt*/Y catalysts produce the high amount of light olefin yield.

For LPG production, the successive impregnation catalysts give higher LPG yield than the co-impregnation catalysts, so the successive impregnated catalysts may have selectivity to produce C_3 and C_4. The catalyst with Pd dispersed on Pt does not produce C_1-C_2 because of the high dispersion of Pd in the catalyst, which prevents from a higher contact of the reaction intermediates with Pt (Roldan *et al.*, 2008).

The LPG yield of the successive impregnated catalysts is also higher than the co-impregnated catalysts (Figure 4.6b). The Pd-Pt*/Y catalyst at α_{Pd} = 0.2 gives the highest LPG yield; after that, the yield decreases with increasing α_{Pd}. The LPG yield of Pd*-Pt/Y catalysts gives similar trend to the Pd-Pt*/Y catalysts. The Pd*-Pt/Y catalysts produce the highest LPG yield at α_{Pd} = 0.4. For co-impregnated catalysts, the LPG yield is very low as compared to all of the catalysts. α_{Pd} = 0.6 of the Pd-Pt/Y catalyst gives the lowest LPG yield.

The Pd/Y catalyst is suitable for light olefins production. The catalysts prepared by successive impregnation with loading Pt first are also suitable for LPG production, especially at α_{Pd} = 0.2.

All of the results indicate that the Pd-Pt*/Y catalysts at α_{Pd} = 0.2 and 0.8 are the best catalysts for producing the oil with high saturated hydrocarbon and low sulfur and aromatic contents. And, they also produce a high LPG yield. The co-impregnation catalyst at α_{Pd} = 0.6 also has a high catalytic activity because it produces the high amount of liquid product with moderate saturated hydrocarbons, and the low amount of polar-aromatics and sulfur in the liquid product. But, it produces very low gas content.

## 4.2 Characterization of Pd and Pt Bimetallic Catalysts

This part discusses the characterization of the bimetallic catalysts by using several techniques such as TPR, TEM, H_2 chemisorption, and elemental analysis. The characterization data can help explaining the effect of bimetallic catalysts to the catalytic activity.
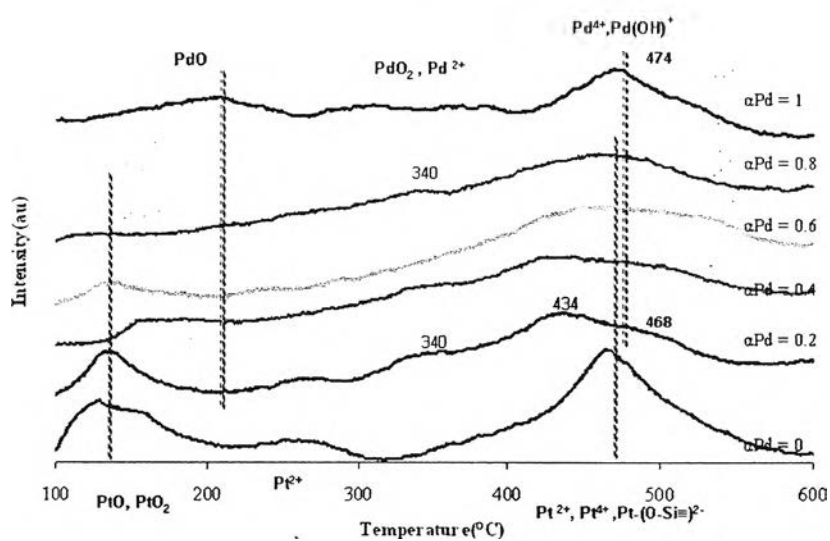
4.2.1 Bimetallic Interaction

The TPR curves of the catalyst samples are shown in Figures 4.6a – 4.6c. The several metal oxide species are reduced at different temperatures depending on the oxidation states, the location of metal on the zeolite, and/or the interaction between two metals.
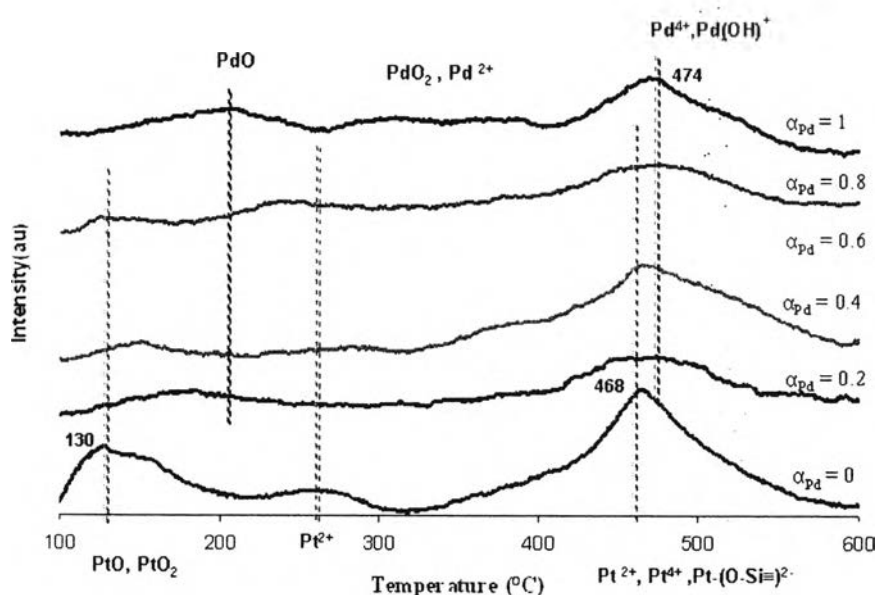
(a)
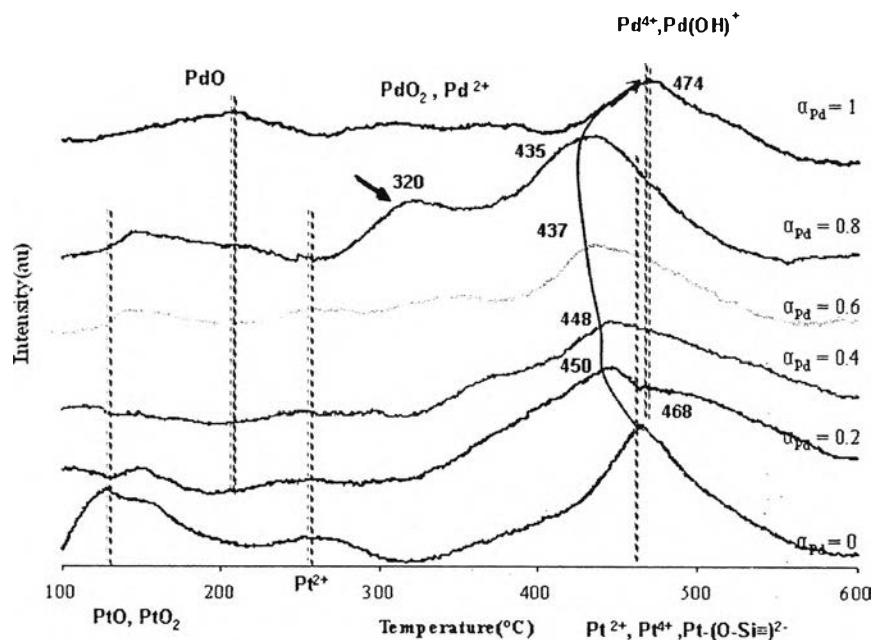
(b)

(c)

Figure 4.7 TPR profiles of bimetallic catalysts: **(a)** Pd-Pt/Y, **(b)** Pd*-Pt/Y, and **(c)** Pd-Pt*/Y catalysts.

The TPR curve of Pt/Y catalyst consists of a broad band at 105 °C to 220 °C, which correspond to PtO and PtO_2 dispersed on the external surface

(Castano et al., 2007); two reduction bands at 230 °C to 315 °C, which correspond to Pt^{2+} ion-exchange in the zeolite channel (Roldan et al., 2008); and a broad reduction peak at 330 – 550 °C with the maximum at 468 °C, which corresponds to Pt^{4+} ion exchange inside the zeolite and Pt^{2+} ions coordinated to silanol groups forming Pt-$(O-Si\equiv)^{2-y}$ species (Ho et al., 1998). For the Pd/Y catalyst, The TPR curve consists of the broad reduction band at 125 °C to 260 °C, which corresponds to PdO located in the zeolite framework; a board band at 270 °C to 400 °C, which corresponds to PdO_2 residing on the external surface and Pd^{2+} ion exchange; and the reduction broad at 410 – 540 °C with the highest peak at 474 °C and a shoulder corresponding to Pd^{4+} located in the super cage or sodalite cage (De Lucas et al., 2005) or $Pd(OH)^+$ strong interact to acid zeolite (Zheng et al., 2008).

Figure 4.7a shows the TPR curves of the catalysts prepared by co-impregnation. The reduction profiles are the combination of the profiles of the monometallic catalysts. The reduction curves at low temperatures (100 °C – 230 °C) show a broad band at 110 °C – 300 °C, which corresponds to the reduction of PdO, PtO, and PtO_2. The Pd ratio affects to the reducibility of bimetallic catalysts (Medrano et al., 2009). The profiles exhibit very broad reduction. Then, it can be implied that the added two metals may change the particle size. A broad band ranging at 230 °C to 400 °C, which corresponds to PdO_2 located in the zeolite channel and Pt^{2+}, Pd^{2+} ion exchange on the zeolite surface. A shoulder in the temperature range from 320 °C to 400 °C corresponds to Pt^{2+} and Pd^{2+}. At high temperatures (above 400 °C), the profiles show the board band with a similar peak to individual reduced metal (either Pt/Y or Pd/Y). The profiles do not show bimetallic interaction.

As mentioned earlier, α_{Pd} = 0.6 of the co-impregnated catalysts has the high catalytic activity for producing the liquid product with the high amount of saturated HCs. The TPR pattern of this catalyst exhibits the peaks representing the two active monometallic sites without new species.

The reduction profiles of Pd*-Pt/Y catalysts are shown in Figure 4.7b. The peak at around 130 °C of every catalysts shifts to higher temperatures (around 145 °C), which corresponds to the interaction of PtO_2 with the support on the external surface. The shoulder (around 350 °C to 375 °C) shifts to lower

temperatures (320 °C) with increasing α_{Pd}. The profiles at higher temperatures show that the peak shifts from around 470 °C to lower temperatures corresponding to strong interaction between two metals. It can be suggested that the degree of interaction between two metals increases with increasing α_{Pd}. For this case, Pd was introduced first and occupied the surface of the support (hydroxyl nest). Then, Pt is loaded in the second stage; therefore, it seems to modify the Pd phase (Roldan et al., 2008). These results suggest that Pt and Pd probably have strong interaction during the reduction, leading to the decrease in the metal-support interaction (Jiang et al., 2007), and then, make the reduction peak shift to lower temperatures. The increasing α_{Pd} can increase the metal-metal interactions; as a result, the peak shifts to lower temperatures. Hence, these catalysts exhibit the new species from strong metal-metal interaction.

From the liquid product yields (Figure 4.1) and saturated hydrocarbon yields (Figure 4.2), the synergy between the Pd and Pt of the Pd*-Pt/Y catalysts has the effect on both quantity and quality products, but is not responsible for the higher catalytic activity over the Pd-Pt*/Y catalysts. So, it implies that the new species (from M-M interaction) slightly enhance the catalytic activity to produce saturated hydrocarbons, but highly improve C-S-C bond cracking activity.

The TPR curves of Pd-Pt*/Y catalysts (Figure 4.7c) are similar to those of Pd-Pt/Y catalysts. The profiles at low temperatures show the reduction of PtO and PtO_2, except α_{Pd} = 0.8, which gives the wide band from 130 °C to 550 °C. The shoulder of a Pd-Pt*/Y catalyst around 340 °C corresponds to the Pt^{2+} and Pd^{2+} ion exchanged on the zeolite. But the shift of shoulder to lower temperatures exhibits the some interaction between two metals. Only α_{Pd} = 0.2 shows the peak shift to lower temperatures, which indicates some interaction between the two metals. Pt is introduced in the first place, forming Pt coordinate silanol groups (hydroxyl nest). And in the second stage, Pd is next loaded and located at the unoccupied locations, which might weakly react with the Pt phase, so the metal-metal interaction of the Pd-Pt*/Y catalysts is stronger than that of the Pd*-Pt/Y catalysts. So, at α_{Pd} = 0.2, the monometallic sites and new species from weak bimetallic interaction were observed. But, at α_{Pd} = 0.8, very broad band (130 – 550 °C) appears, corresponding to the

reduction of Pt and Pd species and the reduction of new species from weak bimetallic interaction from different particle sizes.

From the saturated HCs yield (Figure 4.2), polar aromatic yield (Table 4.3), and sulfur content in oil (Figure 4.4), the Pd-Pt*/Y catalysts at α_{Pd} = 0.2 and 0.8 have high activity to produce highly-stable oil products. These catalysts exhibit the new species (weak bimetallic interaction) and the individual monometallic species. Hence, these catalysts can enhance the hydrogenation and hydrogenolysis activity to produce high saturated HCs yield and the low amount of aromatics and sulfur contents.

4.2.2 Metal Dispersion, Metal Particle Size, and Size Distribution

The metal particle size and metal dispersion are shown in Table 4.4. The TEM images and size distribution graphs are presented in Figures 4.8a – 4.8c. The metal dispersion and metal particle size can reveal the activity of the catalysts. The average particle size (d_{VA}) is determined by using the formula; $d_{VA} = \Sigma nd^3/\Sigma nd^2$ (d refers to particle size (nm), and n refers to the number of particles of each size), as shown in the Table 4.4. The average particle size was determined from accounting for more than 250 particles. The images consist of black points referring to metal particles, which are on the top of lighter and bigger zeolite particles, where, depending on the contrast, the zeolite plane becomes evident. The majority of metal particles are located on the zeolite framework because the pore opening of Y-zeolite is very small (7.5 Å^2) (Roldan et al., 2009). EDS has been used to indicate the metal composition of individual particles.

Table 4.4 Metal particle size and the metal dispersion of catalyst samples

| Catalyst samples	α_{Pd}	Dispersion[1] (%)	Particle size[2] (nm)
Pt/Y	0	37.2	2.79
Pd/Y	1	20.5	7.52
Pd-Pt/Y	0.2	33.1	6.50
	0.4	30.2	6.80
	0.6	34.0	5.33
	0.8	22.7	8.70
Pd*-Pt/Y	0.2	32.8	5.70
	0.4	34.8	5.67
	0.6	26.1	7.02
	0.8	27.9	6.39
Pd-Pt*/Y	0.2	41.6	6.00
	0.4	29.7	8.82
	0.6	26.1	9.38
	0.8	31.3	7.33

[1] determined by H_2 chemisorption

[2] determined by TEM (Volume-area mean diameter)

The results show that the average particle size of Pt/Y and Pd/Y is 2.65 and 6.3 nm, respectively. The metallic particle sizes of Pt/Y catalyst are very smaller than the Pd/Y catalyst, and therefore Pt metals are highly dispersed on the Y-zeolite than Pd metals as indicated by the H_2 chemisorption. As a result, this fact suggests that the Pt atoms are less mobile than Pd atoms because a Pt atom has larger size than a Pd atom (De Lucas et al., 2005). Then, it is easy to show Pd cluster and the high anchor of Pt to protons, leading to high metal dispersion.

The metal particle size of the Pd-Pt/Y catalysts increases with the increasing α_{Pd}, but α_{Pd} = 0.6 has the smallest size (5.33 nm) and narrow size distribution in the range of 3 – 7 nm. Moreover, α_{Pd} = 0.6 also has high metal dispersion (34.0 %). The catalysts prepared by successive impregnation with loading Pd first have new species from strong bimetallic interaction. The lower α_{Pd} shows the smaller particle size than the higher α_{Pd}. And α_{Pd} = 0.4 has the smallest particle size (5.67 nm), and has size distribution in the range of 3 – 8 nm. The size of the metal particles observed in Pd-Pt*/Y catalyst is bigger than those of the other catalysts. It probably causes the emerging new species from weak metal-metal interaction. The metal particle size of Pd-Pt*/Y catalyst at α_{Pd} = 0.2 is the smallest size (6 nm), and

the metal are distributed in the range of 3 − 9 nm. Also, this catalyst has the highest metal dispersion (41.6 %). Increasing α_{Pd} up to 0.6 can affect to the increase of particle size. And at $\alpha_{Pd} = 0.8$, the particle size becomes small again (7.33 nm). This catalyst has wide size distribution in the range of 3 − 13 nm, and has high metal dispersion (31.3 %).
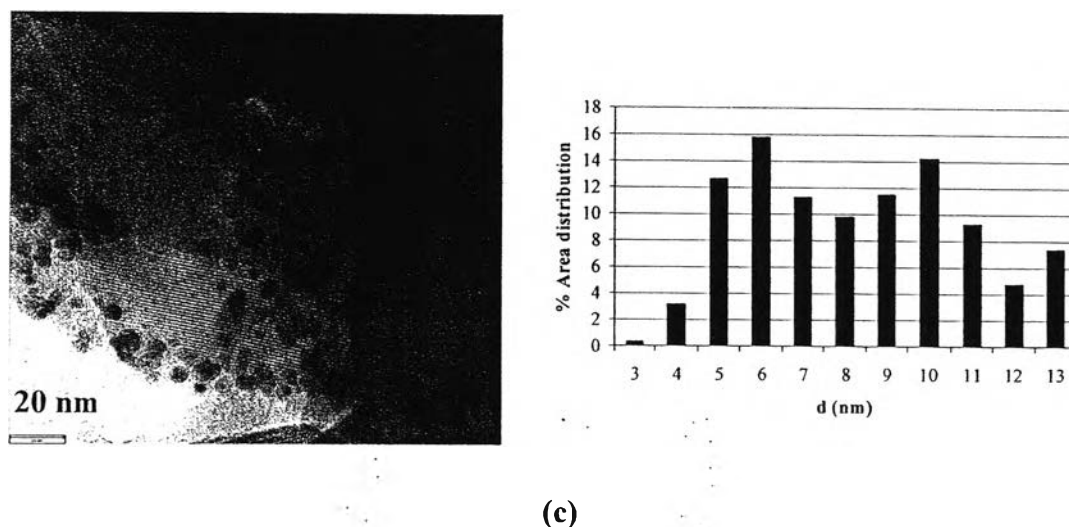

(a)

(b)

(c)
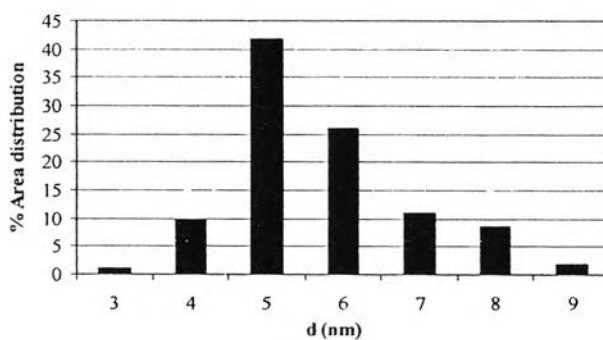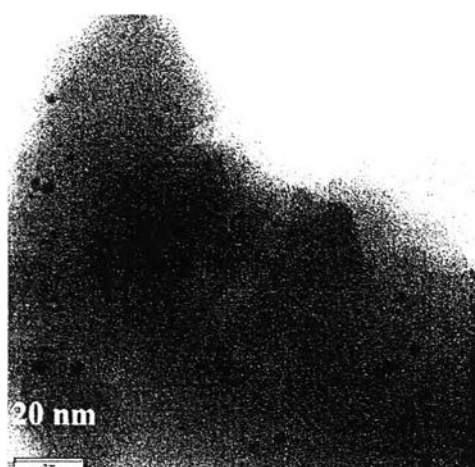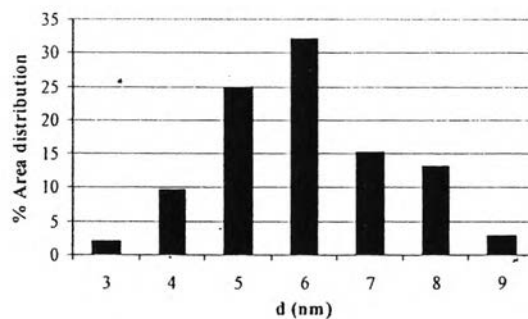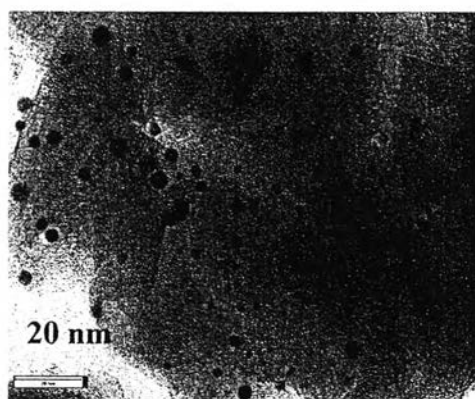
Figure 4.8 TEM images and the size distribution of the bimetallic catalysts: **(a)** Pd-Pt/Y at α_{Pd} = 0.6, **(b)** Pd-Pt*/Y at α_{Pd} = 0.2, and **(c)** Pd-Pt*/Y at α_{Pd} = 0.8.

The Pd-Pt/Y catalyst at α_{Pd} = 0.6 produces the high amount of oil product because the addition amount of Pd in Pt on the acid zeolite improves metal dispersion, and reduces cracking mechanism (Blomsma *et al.*, 2008). This catalyst exhibits the high dispersion of two metals and has uniform particle sizes. The formation of small particles and uniform size distribution are supposed to increase the activity (Kim *et al.*, 2005). So, it has high hydrogenation and hydrogenolysis activity to produce oil with high saturated compounds and low sulfur contents (Barrio *et al.*, 2003).

The Pd-Pt*/Y catalysts at α_{Pd} = 0.2 and 0.8 have high catalytic activity, because these catalysts have high metal dispersion, small metal sizes, wide size distribution, and new species from weak bimetallic interaction. Then, they have high hydrogenation and hydrogenolysis activity to produce oil with high saturated HCs, low sulfur and aromatic contents. These effects were attributed to the higher dispersion of supported particles. Moreover, the wide size distribution also affects to catalytic activity. The larger particle sizes favor to hydrogenation reaction due to relatively less edge and tightly sites (Niquille-Röthlisberger and Prins, 2006). The hydrogenation pathway most probably occurs by ¶-adsorption of the molecule on several metal atoms, whereas hydrogenolysis needs σ-adsorption from the S atom of the reactant on one active site, which has small particle sizes (Niquille-Röthlisberger

and Prins, 2007). The new species on Pd-Pt*/Y catalysts show higher catalytic activity than those of Pd*Pt/Y catalysts.

4.2.4 Sulfur Tolerance and Coke Deposition

The typical reasons on the deactivation of noble metal supported catalysts are sulfur poisoning and coke formation.

In the condition where sulfide compounds are in the process, the monometallic can deactivate by sulfur poisoning (Jaqquin *et al.*, 2004). Sulfur poisoning occurs from sulfur atom adsorbed on the metal sites. Then, the sulfur adsorbed metal sites can not activate. But, the bimetallic catalyst can continuously activate the reaction because they have stronger sulfur resistance than single metal catalysts (Rousset *et al.*, 2000). The factor that can enhance the sulfur tolerance is the metal-metal interaction leading to form the electron deficiency on the metal site, as a result of reducing the sulfur-metal adsorbed strength (Pawalec *et al.*, 2002).

The bimetallic (Pd-Pt) catalysts have higher sulfur tolerance than the monometallic catalysts (Rousset *et al.*, 2000). However, the sulfur tolerance of the bimetallic Pd–Pt catalysts was influenced by several factors, such as the preparation methods, new active sites formation, Pd–Pt particle sizes, and interactions between the Pd–Pt particles and supports, etc. One possible explanation of the electronic effect is the formation of electron-deficient Pt results from bimetallic Pd–Pt interactions (Jaqquin *et al.*, 2004). The decreasing interaction between sulfur and metal on the surface can help to enhance sulfur tolerance.
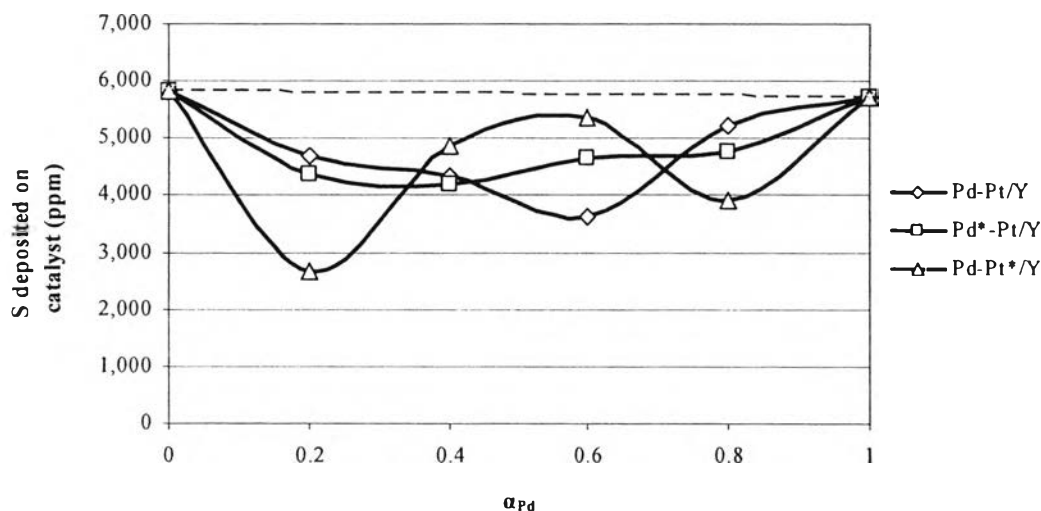
Figure 4.9 Sulfur deposition on the bimetallic catalysts.

The sulfur deposition on the catalysts is determined by using an elemental analyzer, as shown in Figure 4.9. All of the bimetallic catalysts show the lower amount of sulfur deposition on the catalyst than the monometallic catalysts. It can be implied that the bimetallic catalysts have high sulfur resistance.

As shown in Figure 4.9, the deposition sulfur on co-impregnated catalyst decreases with increasing α_{Pd}, and has the lowest sulfur content at $\alpha_{Pd} = 0.6$ (3,633 ppm). After that after increasing α_{Pd} to 0.8, the amount of sulfur deposition starts to increase. The trend of S deposition on the Pd*-Pt/Y catalyst shows that the amount of sulfur slightly decreases with increasing α_{Pd} to 0.4. This ratio has the lowest amount of sulfur on the catalyst (4,202 ppm); and at the higher Pd contents of the catalysts ($\alpha_{Pd} = 0.6$ and 0.8), the amount of sulfur deposition is higher as well. The Pd-Pt*/Y catalysts, which have new species, give the lowest sulfur deposition at $\alpha_{Pd} = 0.2$ (2,672 ppm). Furthermore, the α_{Pd} up to 0.4 and 0.6 present the increase of sulfur deposition; and at $\alpha_{Pd} = 0.8$, the sulfur deposition decreases again (3,922 ppm). The Pd-Pt*/Y catalyst at $\alpha_{Pd} = 0.2$ has the lowest the sulfur deposition (highest sulfur tolerance) as compared to all of catalysts. Then, the Pd-Pt*/Y catalysts at $\alpha_{Pd} = 0.2$ and 0.8 have high sulfur tolerance due to new specie formation. And the Pd-Pt/Y catalyst at $\alpha_{Pd} = 0.6$ also has high catalytic activity due to the low amount of sulfur deposition.
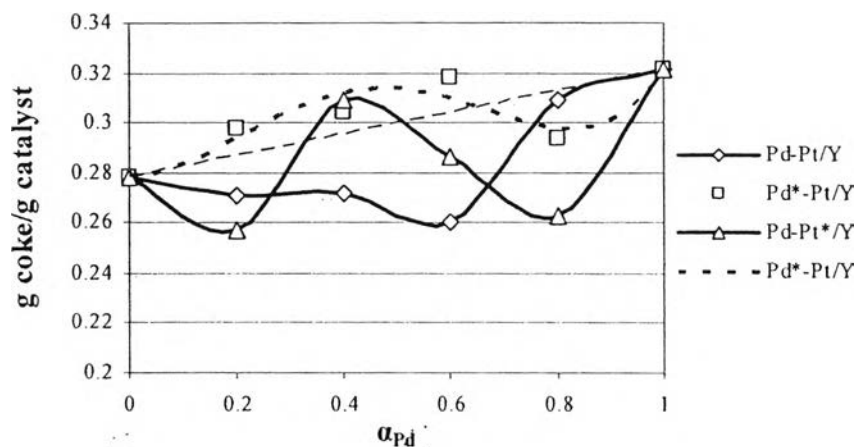
Figure 4.10 Coke formation on the bimetallic catalysts.

The deactivation of catalysts by coke deposition occurs from cracking reaction. Moreover, the increase of sulfur adsorbed on the metal atoms can increase coke formation. Using bimetallic catalysts gives the coke formation that is not much different to monometallic catalyst because the coke formation occurs from acid sites of the zeolite support (Figure 4.10). The lower amount of coke formation of bimetallic catalysts suggests that the high sulfur tolerance and high H-transfer help to reduce coke deposition by reducing S-induced coke and hydrogen spill-over (Lee and Rhee, 1998).

All of the co-impregnated catalysts have lower coke formation than the monometallic catalysts. The Pd-Pt/Y catalysts at α_{Pd} = 0.2 to 0.6 have low coke contents (in the range of 0.26 − 0.27 $g_{coke}/g_{catalyst}$), and α_{Pd} = 0.6 has the lowest coke deposition on the catalyst (0.26 $g_{coke}/g_{catalyst}$). When the α_{Pd} increases up to 0.8, the catalysts have high coke formation again. The successive impregnation catalysts with loading Pd first have the amount of coke deposition closed to that on the monometallic catalysts (0.28 − 0.32 $g_{coke}/g_{catalyst}$). The coke formation insignificantly increases with increasing α_{Pd}. It can imply that the new species from strong bimetallic interaction do not inhibit coke formation. The Pd-Pt*/Y catalysts have the good inhibition on coke formation. These catalysts at α_{Pd} = 0.2 and 0.8 have new species which can prevent coke formation (about 0.26 $g_{coke}/g_{catalyst}$).

The Pd-Pt/Y catalyst at α_{Pd} = 0.6 and the Pd-Pt*/Y catalyst at α_{Pd} = 0.2 and 0.8 are not only have low deposited sulfur. They also have low coke

formation. It can be suggested that these two catalysts have low deactivation and high catalytic activity in the longer period than the other catalysts.